Acetaldehyde Detection Using Chemiresistive-Based Gas Sensors

Subjects: Nanoscience & Nanotechnology

Contributor: Ali Mirzaei, Hyoun Woo Kim, Sang Sub Kim, Giovanni Neri

Volatile organic compounds (VOCs) are among the most abundant air pollutants. Their high concentrations can adversely affect the human body, and therefore, early detection of VOCs is of outmost importance.

Keywords: acetaldehyde ; chemiresistive gas sensor ; nanostructured metal oxide ; sensing mechanism

1. Introduction

By definition, volatile organic compounds (VOCs) are organic compounds with a low boiling point, (50–100 °C to 240–260 °C) and with saturation vapor pressures higher than 102 kPa at 25 °C [1]. They are air pollutants and mostly are emitted from industrial factories and vehicles. They accelerate the formation of secondary organic aerosols, and under oxidized conditions, they will convert them to particles [2]. Accordingly, they cause different environmental problems and also have detrimental effects on human health [3].

Aldehydes are a class of VOCs that are highly reactive and odorous. They are one of the most common sources of pollution in air because they are not only used in many chemical adhesives such as cigarette adhesives [4] but also are produced in many industrial processes or incomplete combustions [5]. In particular, they can be formed as a product of incomplete wood combustion in fireplaces and woodstoves, pulp and paper factories, internal combustion engines and turbines, and vehicle exhaust fumes [6]. Formaldehyde (HCHO) and acetaldehyde (CH_3CHO) are considered two of the most important aldehydes [7][8]. They are known as carcinogenic and probably carcinogenic agents, respectively [9][10].

Acetaldehyde, with the systematic name of ethanal [11], is a small molecule comprising of only four hydrogen atoms, two carbon atoms and one oxygen atom with a low molecular weight (44.05 g/mol) [12], as shown in **Figure 1**. It has an aroma like oranges, low boiling point (20.2 °C), and high solubility in water and lipids [13]. The indoor sources of acetaldehyde include laminates, building materials, wood ceilings, wooden varnished, etc., while its outdoor sources include power plants, wood, trash, oil and gas extraction, cement kilns, refineries, and automobile exhausts [14]. It is also the most abundant carcinogen of tobacco smoke [15]. Acetaldehyde is widely employed to produce acetic acid, acetate esters, pentaerythritol, and pyridine bases [16]. In addition, it is used in the dairy industry as a synthetic flavoring component and food additive [17].

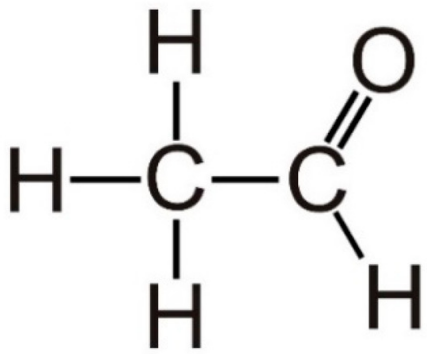

Figure 1. Structure of acetaldehyde.

Acetaldehyde is also a highly toxic compound [18]. The effects of acetaldehyde on the human body include eye irritation, headache, vomiting, liver diseases, and detrimental effects on the throat, skin, and the respiratory tract [19][20][21]. In particular, because of the pungent odor of acetaldehyde, it is extremely irritating at concentrations above 50 ppm [14]. In addition, it can be a cause of sick building syndrome, so-called SBS, even at ppb levels [22][23]. Acetaldehyde has a strong

electrophilic nature and can damage DNA in humans, and it is considered as a possible human carcinogen [24][25]. Furthermore, it can easily react with Vitamin B1, leading to B1 deficiency. Accordingly, it can cause mental illness, visual disturbances, and poor memory in human beings. To avoid such problems, 100 ppm as a permissible exposure limit of acetaldehyde has been proposed [26].

2. Chemiresistive Gas Sensors

Nowadays, gas sensors are widely utilized in different areas including public safety, industrial processes, domestic safety, underground mining, and monitoring of environmental pollution and air quality in vehicles [27]. So far, different types of gas sensors such as surface acoustic wave [28], optical [29], gasochromic [30], thermoelectric [31], electrochemical [32]. and chemiresistive [33][34][35] gas sensors for detection of VOCs have been introduced. Among them, chemiresistive gas sensors are very popular owing to their high sensitivity, short response time, high stability, reproducibility, simple fabrication and operation, and low cost [36][37][38]. Chemiresistive gas sensors, in which the resistance of the sensing layer changes upon exposure to the target gas, were introduced for the first time about sixty years ago [39]. Depending on the increase or decrease of the resistance and the magnitude of the resistance change, the gas type and its concentration can be estimated [40][41]. In chemiresistive gas sensors, surface area, morphology, chemical composition, and sensing temperature are the main factors affecting the gas response [42][43].

A typical resistive-based gas sensor consists of a sensitive layer that is deposited on the surface of interdigitated electrodes printed on an (a) insulating ceramic, (b) plastic, or (c) Si substrate [44]. A heater can also be used on the back of the substrate to raise the sensor temperature up to desired sensing temperatures. However, in some cases, the sensor will be put in a gas chamber in a tubular furnace, where the temperature can be precisely controlled [45].

2.1. General Sensing Mechanism

Figure 2 schematically shows the acetaldehyde sensing mechanism in both pristine n- or p-type metal oxide chemiresistive sensors. For n-types such as ZnO, SnO_2, initially in air, due to abstraction of the electrons by oxygen species, a so-called electron depletion layer will be created on the surface. Because of this, the resistance in the electron depletion layer is higher than that of the core-region parts of the sensing material (**Figure 2**a,b). Upon exposure to acetaldehyde gas, it reacts with already adsorbed oxygen ions and the released electrons come back to the surface of the gas sensor. As a result, the resistance of the gas sensor increases, leading to the appearance of a sensing signal. For p-type metal oxides, such as CuO and Cr_2O_3 [46], initially in air, due to extraction of the electrons by oxygen species, a hole accumulation layer will appear on the surface of the gas sensor (**Figure 2**c,d). Since in p-type metal oxides the main charge carriers are the holes, the resistance in the hole accumulation layer is lower than the core part. In acetaldehyde atmosphere, the released electrons come back to the surface of the gas sensor, leading to higher resistance of the gas sensor and appearance of a sensing signal. A widely used strategy to enhance the gas sensitivity and selectivity is noble metal decoration. The promising effects of noble metals on acetaldehyde detection, which are known as electronic sensitization and chemical sensitization, respectively [47][48], are schematically shown in **Figure 2**e,f. In electronic sensitization, due to the difference between the work functions of noble metals and metal oxides, often electrons from the sensing layer will be moved to the noble metals to equate the Fermi levels. Therefore, in contact areas between the noble metal and metal oxide, the width of the electron depletion layer increases, leading to greater resistance modulation upon exposure to the acetaldehyde gas. In addition, noble metals can act as catalysts for the decomposition of oxygen molecules and target gases. Therefore, initially the gas will be adsorbed on the surface of noble metals, then it will be decomposed into smaller molecules or atoms, and finally. in a so-called spillover effect, it will be moved to the surface of the neighboring sensing layer. Thus, the noble metals can enhance the sensitivity and selectivity of the gas sensors.

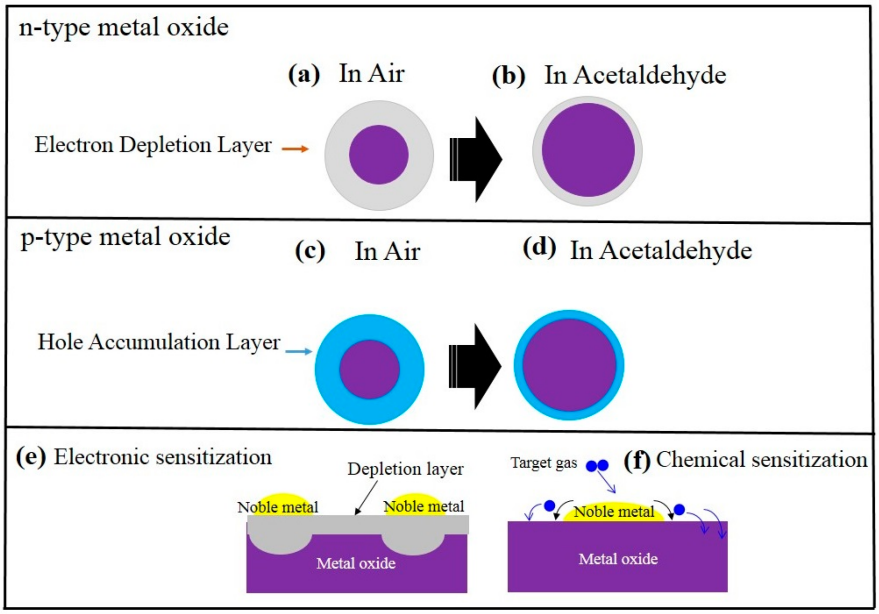

Figure 2. Schematic of acetaldehyde-sensing mechanism in (**a**,**b**) n-type metal oxide and (**c**,**d**) p-type metal oxide. Effect of noble metals on the gas sensing enhancement: (**e**) electronic sensitization (**f**) chemical sensitization.

3. Acetaldehyde Detection Using Chemiresistive-Based Gas Sensors

Traditional strategies to determine the concentration of acetaldehyde are the use of gas chromatography, chemiluminescence, cataluminescence, etc. [49]. Even though such techniques are highly sensitive and accurate, they have some disadvantages for online monitoring, need expert operators, and are bulky as well as expensive. Therefore, sensitive, selective, stable, fast, portable, and simply operated sensors are greatly needed for acetaldehyde detection [6] [50]. For practical applications, an acetaldehyde gas sensor should have following merits: (i) high sensitivity; (ii) high selectivity; (iii) fast dynamics; (iv) long-term stability; (v) reproducibility; (vi) low power consumption; and (vi) low cost. Even though metal-oxide-based gas sensors have most of the above merits, their selectivity and power consumption is a challenge and more research is needed to realize a high acetaldehyde gas sensor for practical applications.

3.1. Morphology-Engineered Nanostructures as Acetaldehyde Gas Sensors

It is well-known that morphology engineering is one of the best strategies to improve the sensing capabilities of metal oxide gas sensors [51][52]. For example, regarding zinc oxide (ZnO), which is one of the most used sensing materials [37][53] [54], different morphologies of ZnO such as nanoparticles (NPs), tetrapods, nanobeads, and nanotubes have been used for gas-sensing studies.

In **Table 1**, some ZnO-based sensors with different morphologies reported for the sensing of acetaldehyde in the literature is presented (**Table 1**). As can be seen, ZnO-based sensors with different morphologies are able to detect low and high concentrations of acetaldehyde gas at different sensing temperatures.

Table 1. Acetaldehyde sensing properties of some ZnO-based gas sensors reported in the literature.

Morphology	Concentration (ppm)	Operating Temperature (°C)	Response (R_a/R_g)	Ref.
Al-doped ZnO	10	500	2250	[55]
ZnO powders	2	450	5.73	[14]
ZnO-$NiCo_2O_4$ nanofibers	100	250	~3	[56]
0.15 mol% Au-ZnO NPs	100	377	~7	[57]

Morphology	Concentration (ppm)	Operating Temperature (°C)	Response (R_a/R_g)	Ref.
ZnO particles	250	400	~45	[58]
ZnO tetrapods	50		47.5	[5]
ZnO nanoaggregates	200	25	~8	[59]
ZnO sheets	1	220	77	[60]
ZnO rods	250	400	5.30	[61]
ZnO flowers			8	[62]
ZnO petals	100		14	
ZnO branched nanorods	10	25	2.85	[26]
Co-doped ZnO branched nanorods	10		800	

For example, ZnO tetrapods with nanosized dimensions were synthesized with a vapor phase method for aldehyde detection [5]. The employed method was catalyst-free and offered very high yield (a few grams were easily produced). On average, the diameter of tetrapods was 60 nm, and their length was 1 mm. The dynamic gas responses were obtained at different temperatures, showing that response/recovery times decreased when the temperature increased. At 400 °C, the sensor revealed a higher response to propionaldehyde (CH_3CH_2CHO) compared to acetaldehyde due to the higher number of electrons returning back to the ZnO when the molecule was completely oxidized [5]:

$$CH_3CHO + 5O^- \rightarrow 2CO_2 + 2H_2O + 5e, \quad (1)$$

$$CH_3CH_2CHO + 8O^- \rightarrow 3CO_2 + 3H_2O + 8e. \quad (2)$$

As shown in the above equations, the reaction of acetaldehyde and propionaldehyde with adsorbed electrons releases five and eight electrons, respectively. Accordingly, the response to acetaldehyde was slightly lower than the response to propionaldehyde. Interestingly, it was found that at T > 350 °C, the response was independent of the relative humidity (RH) value (0–75%).

In another study, flower-like ZnO nanostructures comprised of ZnO nanorods were fabricated through a hydrothermal synthesis method [62]. The hydrothermal method is a cost-effective and versatile method with the possibility of morphology control and is widely used for synthesis of metal oxides for sensing applications [63]. The high response the gas sensor to acetaldehyde compared to CO gas was related to the electron-donating effect of acetaldehyde (10 electrons), which was greater than that of the CO gas (two electrons).

ZnO nanosheets with two-dimensional morphology have attracted a lot of attention for sensing studies due to their high surface areas. In this regard, a fast acetaldehyde gas sensor was introduced using nanosheet-like ZnO nanostructures synthesized through a sonochemical method followed by subsequent etching [64]. The ZnO nanosheets had a high surface area, resulting in an enhanced sensing performance down to the ppb level. At the optimal sensing temperature of 220 °C, the sensor was able to detect even 50 ppb of acetaldehyde gas. Furthermore, the sensor revealed a linear response to acetaldehyde along with fast response and recovery times. The response and recovery times of the sensor to acetaldehyde were 8 and 60 s, respectively, which is very fast for practical applications. In fact, the presence of abundant channels and open space between the ZnO nanosheets accelerated the gas diffusion and decreased the response and recovery times.

References

1. Qi, Y.; Shen, L.; Zhang, J.; Yao, J.; Lu, R.; Miyakoshi, T. Species and release characteristics of VOCs in furniture coating process. Environ. Pollut. 2019, 245, 810–819.
2. Hou, H.; Liu, H.; Gao, F.; Shang, M.; Wang, L.; Xu, L.; Yang, W. Packaging BiVO4 nanoparticles in ZnO microbelts for efficient photoelectrochemical hydrogen production. Electrochim. Acta 2018, 283, 497–508.
3. Katsumata, K.I.; Motoyoshi, R.; Matsushita, N.; Okada, K. Preparation of graphitic carbon nitride (g-C3N4)/WO3 composites and enhanced visible-light-driven photodegradation of acetaldehyde gas. J. Hazard. Mater. 2013, 260, 475–482.
4. He, C.; Jiang, L.-M.; Dai, Y.-H.; Wu, M.-J.; Chen, X.-M.; Cai, C.-Q. Determination of formaldehyde and acetaldehyde in cigarette adhesives by high performance liquid chromatography. Chin. J. Anal. Lab. 2010, 5, 69–72.
5. Calestani, D.; Mosca, R.; Zanichelli, M.; Villani, M.; Zappettini, A. Aldehyde detection by ZnO tetrapod-based gas sensors. J. Mater. Chem. 2011, 21, 15532–15536.
6. Cao, X.; Zhang, Z.; Zhang, X. A novel gaseous acetaldehyde sensor utilizing cataluminescence on nanosized BaCO3. Sens. Actuators B Chem. 2004, 99, 30–35.
7. Delikhoon, M.; Fazlzadeh, M.; Sorooshian, A.; Baghani, A.N.; Golaki, M.; Ashournejad, Q.; Barkhordari, A. Characteristics and health effects of formaldehyde and acetaldehyde in an urban area in Iran. Environ. Pollut. 2018, 242, 938–951.
8. Santana, F.O.; Campos, V.P.; Cruz, L.P.; Luz, S.R. Formaldehyde and acetaldehyde in the atmosphere of Salvador-Ba, Brazil, using passive sampling. Microchem. J. 2017, 134, 78–86.
9. Stefanov, B.I.; Topalian, Z.; Granqvist, C.G.; Österlund, L. Acetaldehyde adsorption and condensation on anatase TiO2: Influence of acetaldehyde dimerization. J. Mol. Catal. A Chem. 2014, 381, 77–88.
10. Kovács, I.; Farkas, A.P.; Szitás, Á.; Kónya, Z.; Kiss, J. Adsorption, polymerization and decomposition of acetaldehyde on clean and carbon-covered Rh (111) surfaces. Surf. Sci. 2017, 664, 129–136.
11. Lachenmeier, D.W.; Salaspuro, M. ALDH2-deficiency as genetic epidemiologic and biochemical model for the carcinogenicity of acetaldehyde. Reg. Tox. Pharm. 2017, 86, 128–136.
12. Raktim Pal Kim, K.-H.; Hong, Y.-J.; Jeon, E.-C. The pollution status of atmospheric carbonyls in a highly industrialized area. J. Hazard. Mater. 2008, 153, 1122–1135.
13. Salaspuro, M. Key role of local acetaldehyde in upper GI tract carcinogenesis. Best Pract. Res. Clin. Gastroenterol. 2017, 31, 491–499.
14. Giberti, A.; Carotta, M.C.; Fabbri, B.; Gherardi, S.; Guidi, V.; Malagù, C. High-sensitivity detection of acetaldehyde. Sens. Actuators B Chem. 2012, 174, 402–405.
15. Haussmann, H.J. Use of hazard indices for a theoretical evaluation of cigarette smoke composition. Chem. Res. Toxicol. 2012, 25, 794–810.
16. Sad, M.E.; Peña, L.G.; Padró, C.L.; Apesteguía, C.R. Selective synthesis of acetaldehyde from lactic acid on acid zeolites. Catal. Today 2018, 302, 203–209.
17. Balagurunathan, B.; Tan, L.; Zhao, H. Metabolic engineering of Escherichia coli for acetaldehyde overproduction using pyruvate decarboxylase from Zymomonas mobilis. Enzym. Microb. Technol. 2018, 109, 58–65.
18. Turner, C.; Španěl, P.; Smith, D. A longitudinal study of ethanol and acetaldehyde in the exhaled breath of healthy volunteers using selected-ion flow-tube mass spectrometry. Rapid Commun. Mass Spectrom. 2006, 20, 61–68.
19. Kanjanasiranont, N.; Prueksasit, T.; Morknoy, D. Inhalation exposure and health risk levels to BTEX and carbonyl compounds of traffic policeman working in the inner city of Bangkok, Thailand. Atmos. Environ. 2017, 152, 111–120.
20. Zhang, X.; Ye, L.; Li, Y.; Zhang, Y.; Cao, C.; Yang, J.; Qi, F. Acetaldehyde oxidation at low and intermediate temperatures: An experimental and kinetic modeling investigation. Combust. Flame 2018, 191, 431–441.
21. Smith, D.; Wang, T.; Sulé-Suso, J.; Španěl, P.; Haj, A.E. Quantification of acetaldehyde released by lung cancer cells in vitro using selected ion flow tube mass spectrometry. Rapid Commun. Mass Spectrom. 2003, 17, 845–850.
22. Tryba, B.; Jafari, S.; Sillanpää, M.; Nitta, A.; Ohtani, B.; Morawski, A.W. Influence of TiO2 structure on its photocatalytic activity towards acetaldehyde decomposition. Appl. Surf. Sci. 2019, 470, 376–385.
23. Itoh, T.; Matsubara, I.; Shin, W.; Izu, N.; Nishibori, M. Preparation of layered organic–inorganic nanohybrid thin films of molybdenum trioxide with polyaniline derivatives for aldehyde gases sensors of several tens ppb level. Sens. Actuators B Chem. 2008, 128, 512–520.

24. Zhang, L.; Zhou, M.; Dong, S. A self-powered acetaldehyde sensor based on biofuel cell. Anal. Chem. 2012, 84, 10345–10349.

25. Verissimo, M.I.; Gamelas, J.A.; Simoes, M.M.; Evtuguin, D.V.; Gomes, M.T.S. Quantifying acetaldehyde in cider using a Mn (III)-substituted polyoxotungstate coated acoustic wave sensor. Sens. Actuators B Chem. 2018, 255, 2608–2613.

26. Mani, G.K.; Rayappan, J.B.B. ZnO nanoarchitectures: Ultrahigh sensitive room temperature acetaldehyde sensor. Sens. Actuators B.Chem. 2016, 223, 343–351.

27. Zhang, J.; Liu, X.; Neri, G.; Pinna, N. Nanostructured materials for room-temperature gas sensors. Adv. Mater. 2016, 28, 795–831.

28. Gao, F.; Boussaid, F.; Xuan, W.; Tsui, C.Y.; Bermak, A. Dual transduction surface acoustic wave gas sensor for VOC discrimination. IEEE Electron. Device Lett. 2018, 39, 1920–1923.

29. Zhao, Y.; Zaghloul, M.; Lilach, Y.; Benkstein, K.; Semancik, S. Metal Organic Framework-Coated Optical VOC Gas Sensor. In Proceedings of the 2018 IEEE Photonics Conference (IPC), Reston, VA, USA, 30 September–4 October 2018.

30. Rizzo, G.; Arena, A.; Bonavita, A.; Donato, N.; Neri, G.; Saitta, G. Gasochromic response of nanocrystalline vanadium pentoxide films deposited from ethanol dispersions. Thin Solid Films 2010, 518, 7124–7127.

31. Rajanna, K. Development of thermoelectric gas sensors for volatile organic compounds. In Proceedings of the SENSORS, 2006 IEEE, Daegu, Korea, 22–25 October 2006; pp. 716–718.

32. Mori, M.; Nishimura, H.; Itagaki, Y.; Sadaoka, Y. Potentiometric VOC detection in air using 8YSZ-based oxygen sensor modified with SmFeO3 catalytic layer. Sens. Actuators B Chem. 2009, 142, 141–146.

33. Kim, J.H.; Lee, J.H.; Mirzaei, A.; Kim, H.W.; Kim, S.S. SnO2 (n)-NiO (p) composite nanowebs: Gas sensing properties and sensing mechanisms. Sens. Actuators B Chem. 2018, 258, 204–214.

34. Mirzaei, A.; Park, S.; Sun, G.J.; Kheel, H.; Lee, C.; Lee, S. Fe2O3/Co3O4 composite nanoparticle ethanol sensor. J. Korean Phys. Soc. 2016, 69, 373–380.

35. Mirzaei, A.; Park, S.; Kheel, H.; Sun, G.J.; Ko, T.; Lee, S.; Lee, C. Acetone Sensors Based on In2O3-Co3O4 Composite Nanoparticles. J. Nanosci. Nanotechnol. 2017, 17, 4087–4090.

36. Mirzaei, A.; Leonardi, S.G.; Neri, G. Detection of hazardous volatile organic compounds (VOCs) by metal oxide nanostructures-based gas sensors: A review. Ceram. Int. 2016, 42, 15119–15141.

37. Mirzaei, A.; Neri, G. Microwave-assisted synthesis of metal oxide nanostructures for gas sensing application: A review. Sen. Actuators B Chem. 2016, 237, 749–775.

38. Mirzaei, A.; Janghorban, K.; Hashemi, B.; Neri, G. metal oxide-shell nanomaterials for gas-sensing applications: A review. J. Nanoparticle Res. 2015, 17, 371.

39. Neri, G. First fifty years of chemoresistive gas sensors. Chemosensors 2015, 3, 1–20.

40. Mirzaei, A.; Kim, J.H.; Kim, H.W.; Kim, S.S. Resistive-based gas sensors for detection of benzene, toluene and xylene (BTX) gases: A review. J. Mater. Chem. C 2018, 6, 4342–4370.

41. Mirzaei, A.; Kim, S.S.; Kim, H.W. Resistance-based H2S gas sensors using metal oxide nanostructures: A review of recent advances. J. Hazard. Mater. 2018, 357, 314–331.

42. Leonardi, S. Two-dimensional zinc oxide nanostructures for gas sensor applications. Chemosensors 2017, 5, 17.

43. Mirzaei, A.; Kim, J.H.; Kim, H.W.; Kim, S.S. How shell thickness can affect the gas sensing properties of nanostructured materials: Survey of literature. Sens. Actuators B Chem. 2018, 258, 270–294.

44. Mirzaei, A.; Janghorban, K.; Hashemi, B.; Bonyani, M.; Leonardi, S.G.; Neri, G. A novel gas sensor based on Ag/Fe2O3 core-shell nanocomposites. Ceram. Int. 2016, 42, 18974–18982.

45. Kim, J.Y.; Lee, J.H.; Kim, J.H.; Mirzaei, A.; Kim, H.W.; Kim, S.S. Realization of H2S sensing by Pd-functionalized networked CuO nanowires in self-heating mode. Sens. Actuators B Chem. 2019, 299, 126965.

46. Kim, H.-J.; Lee, J.-H. Highly sensitive and selective gas sensors using p-type oxide semiconductors: Overview. Sens. Actuators B Chem. 2014, 192, 607–627.

47. Kim, J.H.; Zheng, Y.; Mirzaei, A.; Kim, H.W.; Kim, S.S. Synthesis and selective sensing properties of rGO/metal-coloaded SnO2 nanofibers. J. Electron. Mater. 2017, 46, 3531–3541.

48. Choi, M.S.; Bang, J.H.; Mirzaei, A.; Oum, W.; Na, H.G.; Jin, C.; Kim, S.S.; Kim, H.W. Promotional effects of ZnO-branching and Au-functionalization on the surface of SnO2 nanowires for NO2 sensing. J. Alloy. Comp. 2019, 786, 27–39.

49. Yang, P.; Lau, C.; Liang, J.Y.; Lu, J.Z.; Liu, X. Zeolite-based cataluminescence sensor for the selective detection of acetaldehyde. Lum. J. Biol. Chem. Lum. 2007, 22, 473–479.
50. Abideen, Z.U.; Kim, J.H.; Lee, J.H.; Kim, J.Y.; Mirzaei, A.; Kim, H.W.; Kim, S.S. Electrospun metal oxide composite nanofibers gas sensors: A review. J. Korean Ceram. Soc. 2017, 54, 366–379.
51. Wang, Z.L. Nanostructures of zinc oxide. Mater. Today 2004, 7, 26–33.
52. Ahmad, R.; Majhi, S.M.; Zhang, X.; Swager, T.M.; Salama, K.N. Recent progress and perspectives of gas sensors based on vertically oriented ZnO nanomaterials. Adv. Colloid Interface Sci. 2019, 270, 1–27.
53. Kim, J.H.; Mirzaei, A.; Kim, H.W.; Kim, S.S. Low power-consumption CO gas sensors based on Au-functionalized SnO2-ZnO core-shell nanowires. Sens. Actuators B Chem. 2018, 267, 597–607.
54. Gao, R.; Cheng, X.; Gao, S.; Zhang, X.; Xu, Y.; Zhao, H.; Huo, L. Highly selective detection of saturated vapors of abused drugs by ZnO nanorod bundles gas sensor. Appl. Surf. Sci. 2019, 485, 266–273.
55. Yoo, R.; Li, D.; Rim, H.J.; Cho, S.; Lee, H.S.; Lee, W. High sensitivity in Al-doped ZnO nanoparticles for detection of acetaldehyde. Sens. Actuators B Chem. 2018, 266, 883–888.
56. Liang, Y.; Liu, W.; Hu, W.; Zhou, Q.; He, K.; Xu, K.; Yang, Y.; Yu, T.; Yuan, C. Synthesis and gas-sensing properties of NiCo2O4 shell nanofibers. Mater. Res. Bull. 2019, 114, 1–9.
57. Suematsu, K.; Watanabe, K.; Tou, A.; Sun, Y.; Shimanoe, K. Ultraselective toluene-gas sensor: Nanosized gold loaded on zinc oxide nanoparticles. Anal. Chem. 2018, 90, 1959–1966.
58. Rai, P.; Yu, Y.T. Citrate-assisted hydrothermal synthesis of single crystalline ZnO nanoparticles for gas sensor application. Sens. Actuators B Chem. 2012, 173, 58–65.
59. Srinivasan, P.; Rayappan, J.B.B. Investigations on room temperature dual sensitization of ZnO nanostructures towards fish quality biomarkers. Sens. Actuators B Chem 2019. In press.
60. Fu, X.; Liu, J.; Han, T.; Zhang, X.; Meng, F.; Liu, J. A three-dimensional hierarchical CdO nanostructure: Preparation and its improved gas-diffusing performance in gas sensor. Sens. Actuators B Chem. 2013, 184, 260–267.
61. Rai, P.; Song, H.M.; Kim, Y.S.; Song, M.K.; Oh, P.R.; Yoon, J.M.; Yu, Y.T. Microwave assisted hydrothermal synthesis of single crystalline ZnO nanorods for gas sensor application. Mater. Lett. 2012, 68, 90–93.
62. Rai, P.; Raj, S.; Ko, K.J.; Park, K.K.; Yu, Y.T. Synthesis of flower-like ZnO microstructures for gas sensor applications. Sens. Actuators B Chem. 2013, 178, 107–112.
63. Patil, V.B.; Adhyapak, P.V.; Patil, P.S.; Suryavanshi, S.S.; Mulla, I.S. Hydrothermally synthesized tungsten trioxide nanorods as NO2 gas sensors. Ceram. Int. 2015, 41, 3845–3852.
64. Zhang, S.L.; Lim, J.O.; Huh, J.S.; Noh, J.S.; Lee, W. Two-step fabrication of ZnO nanosheets for high-performance VOCs gas sensor. Curr. Appl. Phys. 2013, 13, S156–S161.